# Nanothermochromic diffraction gratings with giant switching contrast based on the metal-insulator transition of vanadium dioxide

**Johannes Zimmer, Simon A. Haug, Achim Wixforth, Helmut Karl, Hubert J. Krenner**

# Nanothermochromic diffraction gratings with giant switching contrast based on the metal-insulator transition of vanadium dioxide

Johannes Zimmer[a], Simon A. Haug[a], Achim Wixforth[b], Helmut Karl[c], Hubert J. Krenner[a,*]

[a] Emmy Noether Junior Research Group at Lehrstuhl für Experimentalphysik 1 and Augsburg Centre for Innovative Technologies (ACIT), Universität Augsburg, Universitätstr. 1, 86159 Augsburg, Germany
[b] Lehrstuhl für Experimentalphysik 1 and Augsburg Centre for Innovative Technologies (ACIT), Universität Augsburg, Universitätstr. 1, 86159 Augsburg, Germany
[c] Lehrstuhl für Experimentalphysik IV , Universität Augsburg, Universitätstr. 1, 86159 Augsburg, Germany

## ABSTRACT

Nanothermochromic diffraction gratings based on the metal-insulator transition of $VO_2$ are fabricated by site-selective ion-beam implantation in a $SiO_2$ matrix. The studied diffraction gratings were defined (i) directly by spatially selective ion-beam synthesis or (ii) by site-selective deactivation of the metal-insulator transition by ion-beam induced structural defects. The strongest increase of the diffraction efficient was observed at a wavelength of 1550 nm exceeding one order of magnitude for the selectively deactivated gratings. The observed pronounced thermal hysteresis extends down close to room temperature and makes these optical elements well suited for optical memory devices.

**Keywords:** Metal-insulator transition, $VO_2$, diffraction grating, ion implantation

## 1. INTRODUCTION

The metal-insulator transition (MIT) of vanadium dioxide $(VO_2)$[1] has been studied for more than five decades in great detail. The broad interest is on the one hand sparked by the underlying fundamental physical mechanisms[2] on the other hand novel devices are in the focus of applied research. These novel device concepts are utilizing the dramatic variation of both the electrical conductivity[1] and/or optical constants[3-5] which occur at ultrafast timescales.[6,7] For optical devices the thermochromism of $VO_2$ has been employed for diffractive and plasmonic devices as well as metamaterials in both the visible and near-infrared[8-13] and the mid-/far-infrared[14,15] spectral domain.

Here we report on the fabrication of nanothermochromic diffraction gratings based on $VO_2$ nanocrystals (NCs) synthesized by ion-beam implantation and rapid thermal annealing (RTA). We describe two complementary routes for which the grating is defined by position selective (i) NC synthesis or (ii) deactivation of the NCs' MIT. The fabricated devices are characterized by temperature and angular resolved light diffraction at wavelengths used for fiber-optical communication. We demonstrate giant variations of the diffraction efficiencies of the nanothermochromic gratings as the active NCs undergo the MIT.

## 2. SAMPLE FABRICATION

### 2.1 Ion-beam synthesis of vanadium dioxide nanocrystals

Ion-beam synthesis is a versatile technique to fabricate a broad variety of different functional NCs in crystalline and amorphous matrix materials.[16,17] In addition to optically active, emitters such as compound semiconductors,[18] the synthesis of $VO_2$ NCs has been established and improved over the past more than 15 years.[19-25]

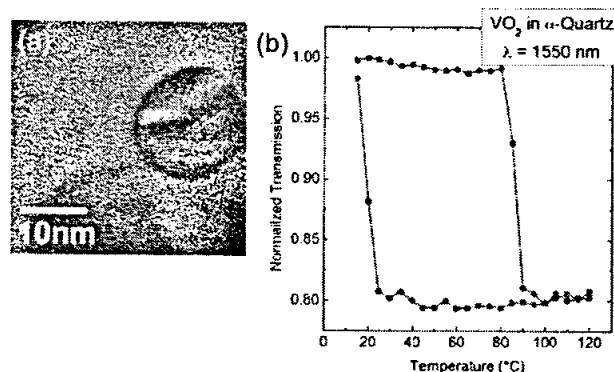*Corresponding author, E-mail: hubert.krenner@physik.uni-augsburg.de

Figure 1. (Color online) Structural and optical characterization of $VO_2$ NCs in *crystalline* quartz – (a) High-resolution transmission electron micrograph (HRTEM) of a single dislocation-free $VO_2$ NC . (b) Normal incidence optical transmission of a 1550 nm laser through an unpatterned layer of $VO_2$ NCs as a function of temperature. The broad thermal hysteresis is characteristic for single-domain $VO_2$ nanosystems.

The ion-beam synthesis of $VO_2$ NCs studied in this work was performed as follows: We start with a two-step implantation process of vanadium ($9 \cdot 10^{16}$ at/cm$^2$ @ 100 keV) and oxygen ($1.8 \cdot 10^{17}$ at/cm$^2$ @ 36 keV). These elements are implanted directly into three different types of substrates: (i) 200 nm thick thermal oxide on a Si wafer for TEM and Raman studies, (ii) 0.5 mm thick fused silica substrate or (iii) α-quartz for diffraction gratings. The $VO_2$ nanocrystals are formed during a 10 min rapid thermal annealing (RTA) step at $T_{RTA} = 1000°C$. For Si – $SiO_2$ and fused silica substrates the temperature was heated up during a 15 s ramp. In contrast to these types of substrates, crystalline quartz required a graded heating profile. Applying the RTA parameters established for Si and amorphous silica substrates, crystalline quartz samples fragmented during the RTA step. We suspect a thermal build up of internal stresses to be the origin of this effect. To avoid this fragmentation, we modified our RTA heating cycle for crystalline quartz substrates which we designed as follows: After an initial ramp to $T_{RTA} = 400°C$ the substrate was kept at this temperature for 30 s. Then we continued with three $\Delta T_{RTA} = 200°C$ temperature steps to the final temperature of $T_{RTA} = 1000°C$. After each temperature step we introduced a settling time of 60 s for the system to stabilize.

We characterized the such synthesized NCs using transmission electron microscopy (TEM). We find that the NCs are positioned 85 nm corresponding well to the projected range of the implanted ions. In addition we found the avaerage NC radius to be 45 nm. The NCs themselves are defect-free and crystalline as can be seen in the high resolution TEM in Figure 1 (a) showing a single NC embedded in crystalline quartz. The MIT can be directly observed by measuring the optical transmission through the NC layer. In Figure 1 (b) we plot the transmission of a $\lambda = 1550$ nm laser as a function of the sample temperature over one thermal cycle starting from $T = 15°C$ to $T = 120°C$. The data is normalized to the start value at $T = 20°C$. The transmission initially remains high as the NCs are in the insulating phase and sharply drops by $\sim 20\%$ at $T = 85°C$ as the NCs undergoe the MIT into the metallic state. This transition temperature is $\sim 17°C$ above the critical temperature of bulk $VO_2$. As the sample temperature is reduced, super-cooling of the metallic phase persist down to room temperature. This broad and asymmetric thermal hysteresis is characteristic for ion-beam synthesized $VO_2$ NCs[19, 22] and points to a monodomain system of either insulating or metallic phase.[26]

## 2.2 Deactivation of the MIT by ion-beam induced defects

The MIT of $VO_2$ and its thermal hysteresis can be controlled by introducing metal (W, Ti, Mo) dopings.[4, 27] This approach can be readily implemented also in the ion-beam synthesis of $VO_2$ NCs.[20, 23] Moreover, in addition to such electrically active metal dopants, charge neutral defects can be generated by irradiation with noble gas ions.[24] In particular when applied for high dose implantation with heavy ions such as Ar$^+$, the large defect densities are generated. These defects in turn fully suppress the MIT of $VO_2$ and the NCs remain in an insulator-

like state for all temperatures. For the work presented here Ar$^+$ ions were implanted with a fluence of $7 \cdot 10^{15} \frac{at}{cm^2}$ @ 80 keV.

## 2.3 Nanothermochromic diffraction gratings

**(a) – Direct Synthesis (DS)**

Vanadium / Oxygen

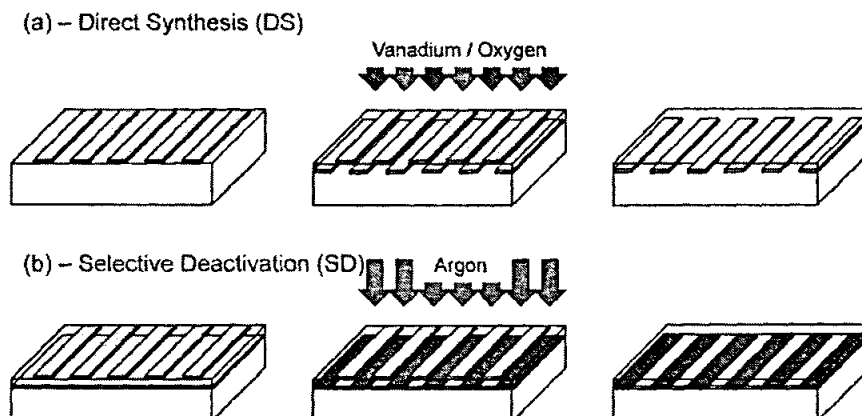**(b) – Selective Deactivation (SD)**

Argon

Figure 2. (Color online) Ion beam fabrication of VO$_2$ nanothermochromic diffraction gratings – (a) Direct synthesis (DS) and (b) selective deactivation (SD).

We present the two different routes, direct synthesis (DS) and selective deactivation (SD), to realize nanothermochromic diffraction gratings in Fig. 2 (a) and (b), respectively. For both approaches we evaporate a 120 nm thick chromium implantation mask on 1 cm × 1 cm fused silica glass substrates (Crystec, Berlin) which is patterned by conventional optical lithography in a lift-off process*. This mask can be completely removed after implantation by a highly selective wet chemical etch.

In the first approach shown in Fig. 2 (a) VO$_2$ nanocrystals are synthesized by implantation of vanadium and oxygen through the chromium mask using the parameters given in subsection 2.1. In this bottom-up approach a RTA step is required after the chromium mask has been removed. We refer to this type of gratings as *directly synthesized* (DS) gratings. For the top-down process shown in panel (b) of Fig. 2 we start with a substrate already containing a homogeneous layer of VO$_2$ nanocrystals. Here the mask protects arrays of nanocrystals during an Ar$^+$ ion implantation step. As described in subsection 2.2, the bombardment with Ar$^+$ ions introduces defects in the VO$_2$ nanocrystals which completely inhibit their MIT. Due to this novel property we refer to this type of gratings as *selectively deactivated* (SD) in the following. † Both types of two gratings are clearly resolved in the optical micrographs of Fig. 3 (a) and (b).

# 3. OPTICAL CHARACTERIZATION

## 3.1 Experimental details

We characterized our gratings using angle-resolved light diffraction as a function of temperature. As light sources we employed commercial diode lasers at three technologically most relevant wavelengths of 980 nm, 1310 nm and 1550 nm. The samples themselves were mounted on a house built double-stage-Peltier temperature-controlled holder in the center of a 25 cm diameter double-stage goniometer. This setup allows for independent tuning of the angle of incidence and detection. The diffracted light was detected with an angular resolution of < 0.5 degrees using an amplified InGaAs photodiode.

---

*Fused silica substrates are required due to the high RTA temperature of $T_{RTA} = 1000°C$.

†For SD gratings no further thermal treatment is required after mask removal. Thus, SD gratings can be readily defined in a "cold" process in contrast to their DS counterparts.
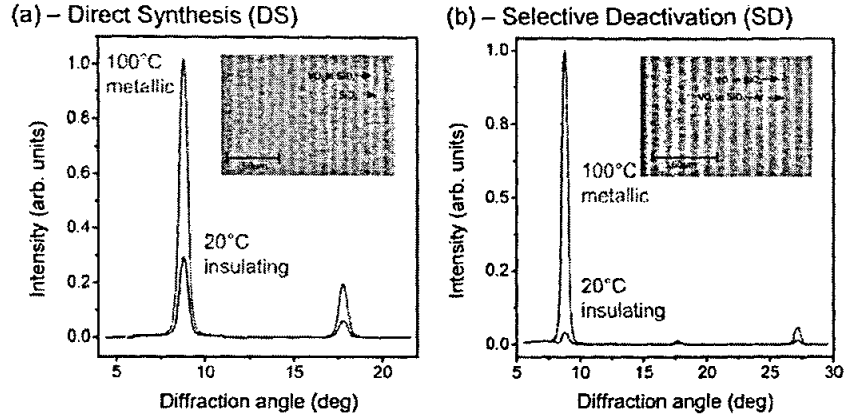
**(a) – Direct Synthesis (DS)**

**(b) – Selective Deactivation (SD)**

Figure 3. (Color online) Nanothermochromic switching of $VO_2$ diffraction gratings - Diffracted light intensity as a function of angle for a DS (a) and SD grating (period $\Lambda = 10$ μm) in the insulting ($T = 20°C$, blue) and the metallic state ($T = 100°C$, red). Optical microscope images of both types of gratings are shown as insets.

## 3.2 Angle resolved light diffraction

### 3.2.1 Normal incidence light diffraction

In Fig. 3 we compare the diffracted light intensity of a DS and SD grating in the insulating phase at room temperature ($T = 20°C$, blue) and in the metallic phase ($T = 100°C$, red) in panels (a) and (b), respectively. The periodicity of both gratings was $\Lambda = 10$ μm with duty cycles of 0.66 ($VO_2 + SiO_2$: $SiO_2$) and 0.5 for the DS and SD grating respectively. These scans were taken under normal incidence from the sample backside using a 1550 nm laser. For both gratings we observe a pronounced increase of the diffracted light intensity as the $VO_2$ nanocrystals undergo their phase transition into the metallic state. This increase of the diffraction efficiency arises from an enhanced dielectric contrast. Since we observe a clear increase, the contribution of the refractive component dominates over contributions from plasmonic losses in the metallic nanocrystals.[28] As a figure of merit we define the switching contrast

$$\eta = I_{metallic}/I_{insulating} \qquad (1)$$

to assess the nanothermochromic switching performance. The most striking difference is observed for the variation of the diffraction efficiencies of the two grating types. Diffraction is pronounced for the DS grating due to the relatively large refractive index contrast between the non implanted $SiO_2$ and the $VO_2$ : $SiO_2$ for both low and high temperatures. As $VO_2$ undergoes the MIT into the metallic state the diffraction efficiency increases corresponding to $\eta \sim 3$ due to the aforementioned enhancement of the refractive index contrast. In strong contrast, the SD grating diffraction is weak at room temperature due to the minute refractive index contrast generated by the $Ar^+$-ion bombardment. As the active $VO_2$ nanocrystals undergo the MIT to the metallic state, their refractive index change results in a giant variation of the dielectric contrast of the grating. This in turn gives rise to the observed giant enhancement of the diffraction efficiency by more than one order of magnitude, $\eta \sim 24$.

### 3.2.2 Incidence angle scans

We further characterized the diffraction properties and thermochromic switching performance of the SD grating in reflection geometry as a function of the angle of incidence. We plot two full scans for the $VO_2$ nanocrystals in the insulating ($T = 15°C$) and metallic phase ($T = 110°C$) as a function of incidence and detection angle in Fig. 4 (a) and (b), respectively. The origin of the detection angle (horizontal axis) is set to that of the directly reflected beam's. In both plots we use identical logarithmic scales for both the vertical intensity axis
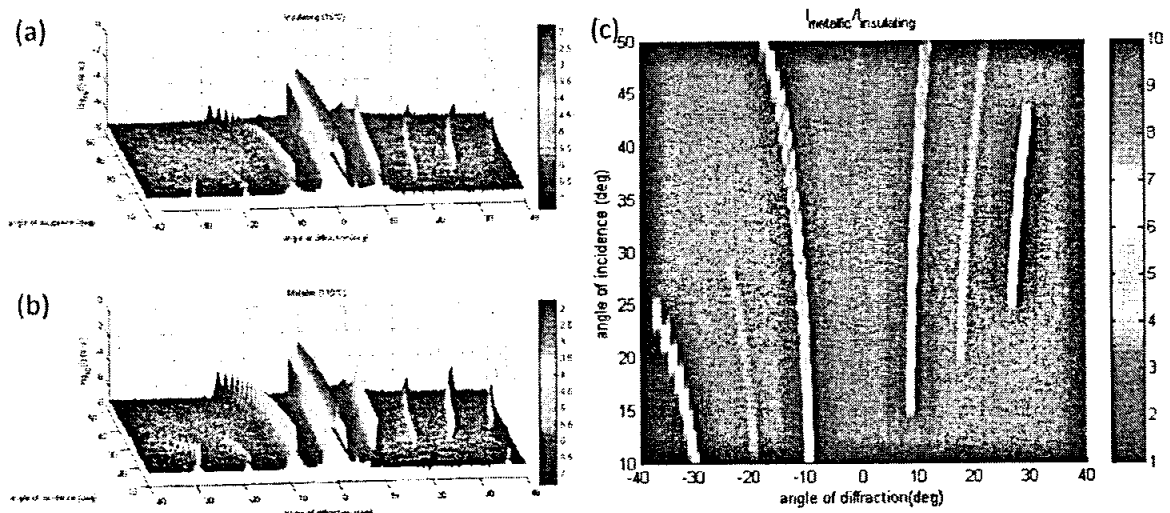
Figure 4. (Color online) Incidence and diffraction angle dependence (a) and (b) Diffracted light intensity of a DS grating in the insulating ($T = 15°C$) and metallic phase ($T = 110°C$) as a function of incidence and detection angle. (c) Switchting contrast ($\eta$) extracted from the data in (a) and (b).

and color code[‡]. Clearly, the nanothermochromic switching is also fully resolved in this geometry for all detected diffraction orders as well as for the directly reflected beam. From these data we extracted the switching contrast, $\eta$, as a function of of incidence and detection angle. This analysis clearly demonstrates that the pronounced nanothermochromic switching is also resolved under reflection geometry with $\eta > 9$ for the principal diffraction orders. While this is reduced by a factor of $\sim 2$ compared to the data recorded in transmission [cf. Fig. 3 (b)], a similar value $\eta \sim 6$ is observed for the next allowed higher diffraction orders. Moreover, we want to point out that for the directly reflected beam the contrast is only minute. This demonstrates that the application of such diffractive optical elements represents a powerful tool to monitor variations of the dielectric properties. Thus this method is not limited to (nano)thermochromism but could be also applied and extended to other systems such as electrochromic materials.

### 3.3 Thermal hysteresis

The well known pronounced thermal hysteresis in nanoscopic $VO_2$ allows the implementation of bistable electronic and optical elements e.g. for memory and storage applications. We studied this feature for our ion beam synthesized $VO_2$ nanothermochromic gratings and find wide hysteresis loops for both directly synthesized and selectively deactivated gratings. The obtained temperature dependencies of switching contrast defined in equation (1) of a DS grating ($DC = 0.66$) and a SD grating ($DC = 0.5$) are plotted for increasing (circles) and decreasing (triangles) temperature and all three wavelengths studied in Fig. 5 (a,b) and (c,d), respectively. In these plots the transition temperature of bulk $VO_2$ is marked by the dashed vertical line. The arrows in panel (b) mark "quantized" switching events which could arise from different switching temperatures of different nanocluster sub-ensembles due to variations of the local strain fields or number of domains. For all samples studied the pronounced hysteresis is asymmetric with respect to $T_C$. Most notably, supercooling of the MIT persists down close to room temperature to $T = 30\ °C$ and $T = 40\ °C$ for the DS and SD gratings, respectively. These observations are also consistent with direct optical transmission experiments reported previously[20] and the data shown in Fig. 1.

---

[‡]For small incidence and positive detection angles (lower right part of plots) the detector blanks out the incident beam and no signal can be detected. The asymmetry with respect to positive and negative detection angles arises from imperfections in the setup alignment for this two-angle geometry.
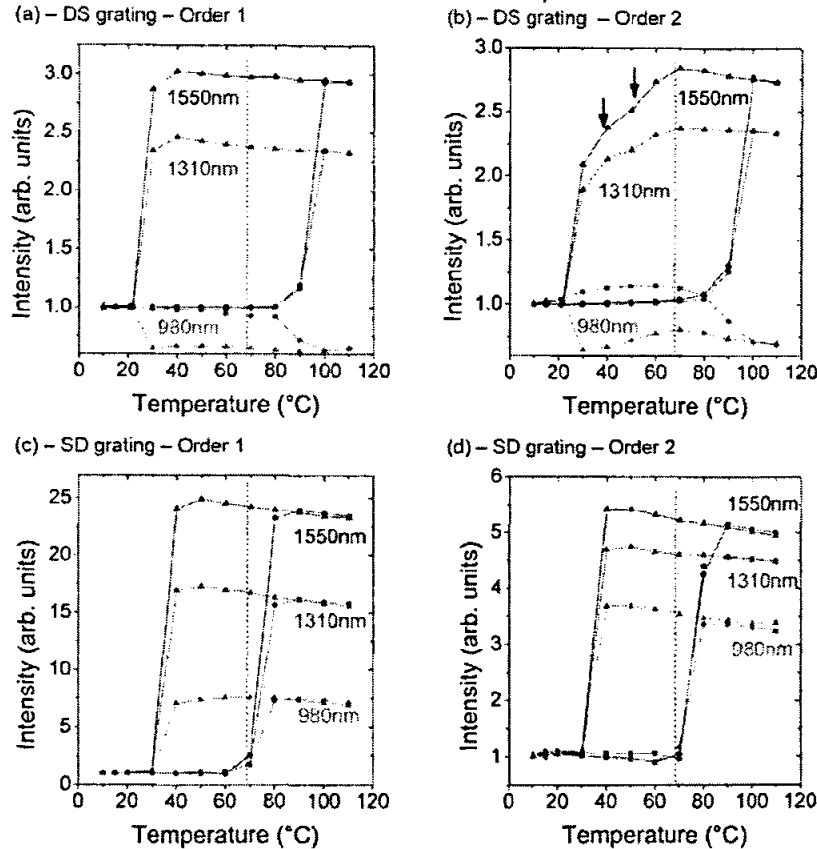
(a) – DS grating – Order 1

(b) – DS grating – Order 2

(c) – SD grating – Order 1

(d) – SD grating – Order 2

Figure 5. (Color online) Thermal hysteresis — Thermal hysteresis of $\eta$ of the principal and secondary diffraction order for DS grating with $DC = 0.66$ (a+b) and a SD grating with $DC = 0.5$ (c+d) for the three wavelength studied. Intensities are normalized to the insulting phase and circles (triangles) correspond to increasing (decreasing) temperature scans. The transition temperature of bulk crystals ($T_C = 68$ °C) is marked by dashed lines.

# 4. CONCLUSIONS

In summary, we realized nanothermochromic ($VO_2$ nanocrystal SiO$_2$) composite diffraction gratings by site selective ion implantation. We fabricated diffraction gratings by this standard semiconductor fabrication technique which exhibit giant switching ratios of more than a factor of 3 for DS and exceeding one order of magnitude for SD gratings. Our technique can be applied to realize a broad spectrum of diffractive planar optical elements e.g. phase lenses or optical memory devices.

# ACKNOWLEDGMENTS

# REFERENCES

1. F. Morin, "Oxides Which Show a Metal-to-Insulator Transition at the Neel Temperature," *Physical Review Letters* 3, pp. 34–36, July 1959.
2. L. Whittaker, C. J. Patridge, and S. Banerjee, "Microscopic and Nanoscale Perspective of the MetalInsulator Phase Transitions of VO$_2$ : Some New Twists to an Old Tale," *The Journal of Physical Chemistry Letters* 2, pp. 745–758, Apr. 2011.

3. H. W. Verleur, A. S. Barker, and C. N. Berglund, "Optical Properties of $VO_2$ between 0.25 and 5 eV," *Physical Review* **172**, pp. 788–798, Aug. 1968.

4. M. Tazawa, P. Jin, and S. Tanemura, "Optical constants of $VO_{1-x}W_xO_2$ Films," *Appl. Opt.* **37**(10), pp. 1858–1861, 1998.

5. W.-T. Liu, J. Cao, W. Fan, Z. Hao, M. C. Martin, Y. R. Shen, J. Wu, and F. Wang, "Intrinsic optical properties of vanadium dioxide near the insulator-metal transition.," *Nano Letters* **11**, pp. 466–70, Feb. 2011.

6. A. Cavalleri, C. Tóth, C. Siders, J. Squier, F. Ráksi, P. Forget, and J. Kieffer, "Femtosecond Structural Dynamics in $VO_2$ during an Ultrafast Solid-Solid Phase Transition," *Physical Review Letters* **87**, pp. 237401–, Nov. 2001.

7. A. Cavalleri, T. Dekorsy, H. Chong, J. Kieffer, and R. Schoenlein, "Evidence for a structurally-driven insulator-to-metal transition in $VO_2$: A view from the ultrafast timescale," *Physical Review B* **70**, pp. 161102–, Oct. 2004.

8. R. Lopez, L. Feldman, and R. Haglund, "Size-Dependent Optical Properties of $VO_2$ Nanoparticle Arrays," *Physical Review Letters* **93**, p. 177403, Oct. 2004.

9. E. Donev, J. Suh, F. Villegas, R. Lopez, R. Haglund, and L. Feldman, "Optical properties of subwavelength hole arrays in vanadium dioxide thin films," *Physical Review B* **73**, p. 201401, May 2006.

10. J. Y. Suh, E. U. Donev, R. Lopez, L. C. Feldman, and R. F. Haglund, "Modulated optical transmission of subwavelength hole arrays in metal-$VO_2$ films," *Applied Physics Letters* **88**, p. 133115, Mar. 2006.

11. J. Zimmer, A. Wixforth, H. Karl, and H. J. Krenner, "Ion beam synthesis of nanothermochromic diffraction gratings with giant switching contrast at telecom wavelengths," *Applied Physics Letters* **100**, p. 231911, June 2012.

12. J. Zimmer, A. Wixforth, H. Karl, and H. J. Krenner, "Erratum: Ion beam synthesis of nanothermochromic diffraction gratings with giant switching contrast at telecom wavelengths [Appl. Phys. Lett. 100, 231911 (2012)]," *Applied Physics Letters* **101**, p. 189901, Nov. 2012.

13. J. D. Ryckman, V. Diez-Blanco, J. Nag, R. E. Marvel, B. K. Choi, R. F. Haglund, and S. M. Weiss, "Photothermal optical modulation of ultra-compact hybrid Si − $VO_2$ ring resonators," *Optics Express* **20**, p. 13215, May 2012.

14. T. Driscoll, S. Palit, M. M. Qazilbash, M. Brehm, F. Keilmann, B.-G. Chae, S.-J. Yun, H.-T. Kim, S. Y. Cho, N. M. Jokerst, D. R. Smith, and D. N. Basov, "Dynamic tuning of an infrared hybrid-metamaterial resonance using vanadium dioxide," *Applied Physics Letters* **93**, p. 024101, July 2008.

15. T. Driscoll, H.-T. Kim, B.-G. Chae, B.-J. Kim, Y.-W. Lee, N. M. Jokerst, S. Palit, D. R. Smith, M. Di Ventra, and D. N. Basov, "Memory metamaterials.," *Science* **325**, pp. 1518–21, Oct. 2009.

16. A. Meldrum, R. F. J. Haglund, L. A. Boatner, and C. W. White, "Nanocomposite Materials Formed by Ion Implantation," *Advanced Materials* **13**, pp. 1431–1444, Sept. 2001.

17. H. Karl, I. Groß hans, and B. Stritzker, "Combinatorial ion beam synthesis of semiconductor nanoclusters," *Measurement Science and Technology* **16**, pp. 32–40, Jan. 2005.

18. A. W. Achtstein, H. Karl, and B. Stritzker, "Field induced photoluminescence quenching and enhancement of CdSe nanocrystals embedded in $SiO_2$," *Applied Physics Letters* **89**, p. 061103, Aug. 2006.

19. L. A. Gea and L. A. Boatner, "Optical switching of coherent $VO_2$ precipitates formed in sapphire by ion implantation and annealing," *Applied Physics Letters* **68**, p. 3081, May 1996.

20. R. Lopez, L. A. Boatner, T. E. Haynes, L. C. Feldman, and J. R. F. Haglund, "Synthesis and characterization of size-controlled vanadium dioxide nanocrystals in a fused silica matrix," *Journal of Applied Physics* **92**(7), pp. 4031–4036, 2002.

21. R. Lopez, T. E. Haynes, L. A. Boatner, L. C. Feldman, and J. R. F. Haglund, "Temperature-controlled surface plasmon resonance in $VO_2$ nanorods," *Optics Letters* **27**(15), pp. 1327–1329, 2002.

22. R. Lopez, T. Haynes, L. Boatner, L. Feldman, and R. Haglund, "Size effects in the structural phase transition of $VO_2$ nanoparticles," *Physical Review B* **65**, p. 224113, June 2002.

23. H. Karl, J. Dreher, and B. Stritzker, "Semiconductor-metal Phase Transition in Doped Ion Beam Synthesized $VO_2$ Nanoclusters," *MRS Proceedings* **1174**, Jan. 2009.

24. H. Karl, J. Peng, and B. Stritzker, "Effects of He-irradiation on the Metal-to-insulator Transition of Vanadium Dioxide Nanoclusters," *MRS Proceedings* **1256**, Jan. 2010.

25. H. Amekura, Y. Nakayama, K. Mitsuishi, and K. Kono, "Formation of metallic vanadium nanoparticles in $SiO_2$ by ion implantation and of vanadium oxide nanoparticles by additional thermal oxidation," *Thin Solid Films* **520**, pp. 5528–5533, June 2012.

26. K. Appavoo, D. Y. Lei, Y. Sonnefraud, B. Wang, S. T. Pantelides, S. A. Maier, and R. F. Haglund, "Role of defects in the phase transition of $VO_2$ nanoparticles probed by plasmon resonance spectroscopy.," *Nano Letters* **12**, pp. 780–6, Feb. 2012.

27. X. Tan, T. Yao, R. Long, Z. Sun, Y. Feng, H. Cheng, X. Yuan, W. Zhang, Q. Liu, C. Wu, Y. Xie, and S. Wei, "Unraveling metal-insulator transition mechanism of $VO_2$ triggered by tungsten doping.," *Scientific Reports* **2**, p. 466, Jan. 2012.

28. M. Rini, A. Cavalleri, R. W. Schoenlein, R. López, L. C. Feldman, J. Richard F. Haglund, L. A. Boatner, and T. E. Haynes, "Photoinduced phase transition in $VO_2$ nanocrystals: ultrafast control of surface-plasmon resonance," *Optics Letters* **30**(5), pp. 558–560, 2005.